Pergamon

Journal of Structural Geology, Vol. 17, No. 10, pp. 1395 to 1405, 1995

0191-8141/95 $9.50+0.00

0191-8141(95)00035-6

Quartz pressure solution: influence of crystallographic orientation

A. BECKER

Ramon Science Center, The Jacob Blaustein Institute for Desert Research, Ben-Gurion University of the Negev, P.O. Box 194, Mizpe Ramon 80600, Israel

(*Received 20 April 1994; accepted* 13 *March* 1995)

Abstract—The present contribution examines the relationship between pressure solution and the crystallographic orientation of detrital quartz in cleaved sandstones which exhibit a high degree of pressure solution. The majority of the detrital grains examined have undergone pressure solution and as a result they have acquired smooth truncated margins along certain cleavage planes. The amount of pressure solution varies significantly among the detrital grains. This analysis indicates that quartz offers variable resistance to pressure solution along different crystallographic directions. Quartz grains with a small angle between *c*-axis and the *Z*-axis of shortening exhibit the least amount of pressure solution, whereas grains with *c*-axes oriented about 50° to *Z* manifest the highest degree of the pressure solution.

INTRODUCTION

During past decades, the nature of cleavage formation has been under intensive study. Pressure solution as a dominant deformational mechanism in cleavage development has been suggested by Durney (1972), Groshong (1975, 1976), Gray (1982), Onasch (1983), Soper (1986), Waldron & Sandiford (1988), Price & Cooper (1990) and Twiss & Moores (1992) amongst others. In sandstones, quartz is the main soluble phase during cleavage development (Groshong 1975, 1976, Onasch 1983). The extent to which quartz is affected by pressure solution depends upon a number of factors, including grain size, roundness, matrix composition, strain rate and temperature (Hobbs 1968, 1985, Renton *et al.* 1969, DeBoer 1977, Houseknecht 1984, 1988, Kazakov 1987, Dewers & Ortoleva 1991). The present contribution deals with the dependence of pressure solution on the crystallographic orientation of detrital quartz grains.

The middle Riphean cleaved sandstones from the Talas Ridge (Kyrgyzstan) were examined and the following remarkable features of their fabrics were noted: (1) the majority of the detrital grains are flattened parallel to the cleavage planes; (2) the grain boundaries are truncated against the cleavage lamellae, but the amount of truncation was found to vary significantly in different grains; and (3) against the background of truncated flattened grains, some equant grains preserve their original detrital shape. The latter grains do not show evidence of pressure solution along sides facing the cleavage, but instead they contain mica beards and fibrous quartz overgrowths in pressure shadows extending parallel to the cleavage. The sizes of these grains vary in shape, ranging from angular to rounded, and are distributed throughout the rock matrix. It seems that the only feature that distinguishes these grains from other detrital grains is their specific orientation in relation to the stress field.

Kamb (1959) found that anisotropic minerals are thermodynamically more stable in some orientations than in other orientations. Thus in an aggregate of grains of different orientations, some grains will tend to dissolve whereas others will tend to grow. In addition, the mechanical properties of quartz vary along different crystallographic directions (Sobolev 1957, Brace 1960, Kazakov 1987). Previous attempts to find a correlation between the degree of pressure solution and quartz grain orientation have been mostly based on the study of the geometry of pressolved contacts in weakly deformed sandstones (e.g. Taylor 1950, Hicks *et al.* 1986). Kennedy (1950) and Hicks *et al.* (1986) suggested that dissolution of quartz is faster along the *c*-axis relative to other crystallographic directions.

In the present contribution the results from the study of quartz pressure solution in four specimens of cleaved sandstone are discussed. It will be shown that the degree of the pressure solution depends on the orientation of quartz grains in relation to the principal axis of shortening.

GEOLOGICAL SETTING

The rocks studied were collected along a section of the Talas Ridge (Tien Shan mountain system, Kyrgyzstan—Fig. 1a). The Talas Ridge is comprised of two main tectonic sheets (Fig. 1b): the Uzunakhmat Sheet (southern) and the Karagoin Sheet (northern). The Uzunakhmat Sheet is composed of middle Riphean rocks (Korolev & Maksumova 1964, Kiselev & Korolev 1981) which have been metamorphosed to greenschist facies (Bakirov & Dobrezov 1972). The metamorphic grade increases southward (Frolova 1982). The Karagoin Block is composed of unmetamorphosed late Riphean, Vendian and early Paleozoic rocks (Korolev & Maksumova 1964, Kiselev & Korolev 1972, 1981, Maksumova 1980). The Uzunakhmat Sheet was overthrust onto the Karagoin Sheet along a system of imbricate

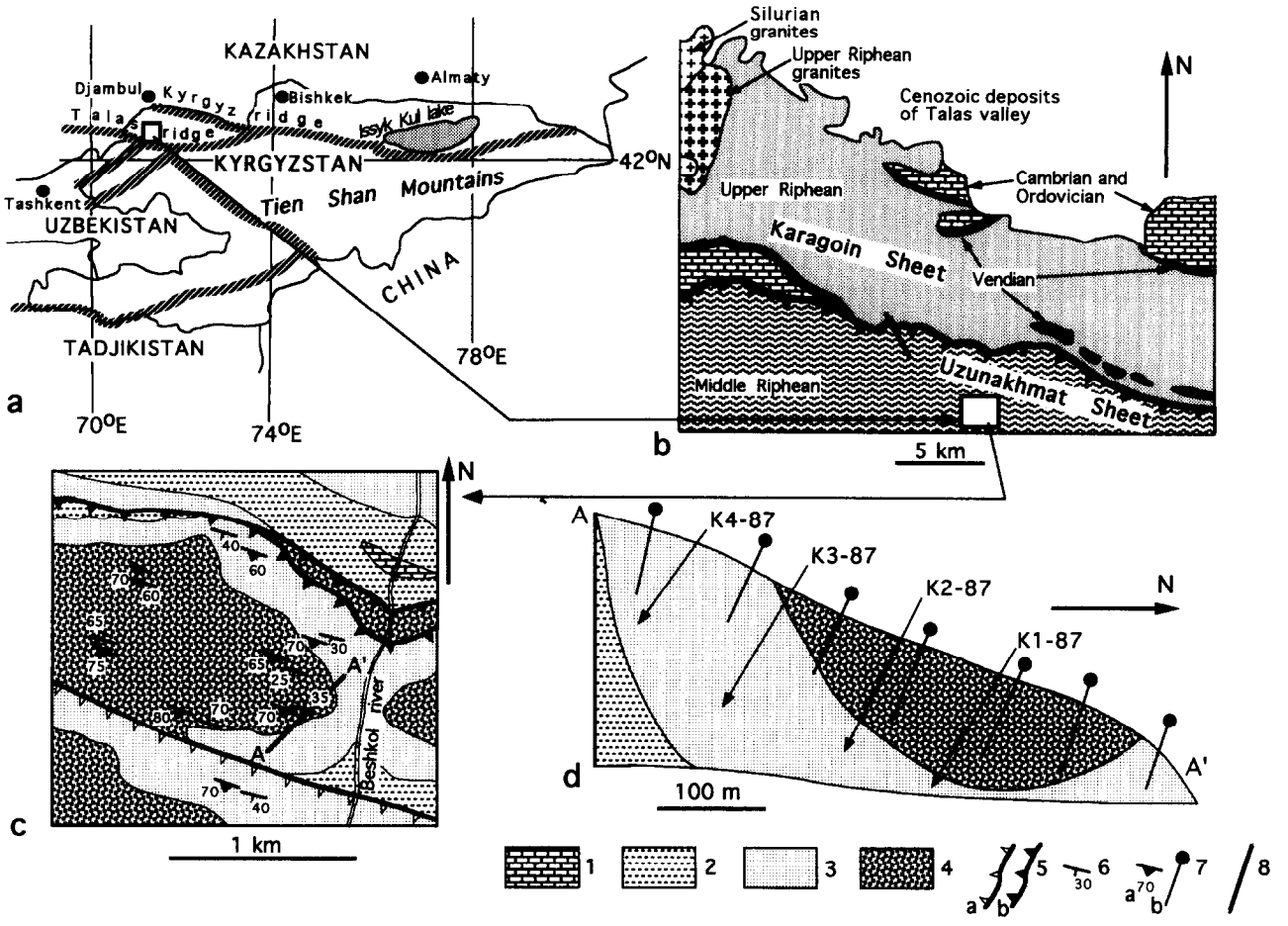

Fig. 1. Geological sketches and location maps of the study area. (a) Regional geographic setting. (b) Simplified geological map showing locations of the main regional tectonic elements. (c) Geological map of the study area showing location of the section. (d) Geological cross-section and location of specimens examined (shown by arrows). Legend for the geological map (c) and cross-section (d): 1, Karabura Formation—intercalations of marble and carbonaceous sandstone; 2–4, Uzunakhmat Formation, 2, Member 1—phyllites with interbeds of sandstone; 3, Member 2—intercalation (2–10 m) of sandstone and phyllitic beds; 4, Member 3—sandstone and microconglomerate; 5, faults: a—reverse faults, b—thrusts; 6, strike and dip of bedding; 7, orientation of cleavage: a—in the map, b—in the section; 8, location of the section.

thrusts between the Late Ordovician and Early Devonian (Becker 1988), whereas the main phase of folding occurred during the end of Riphean times (Kiselev *et al.* 1988). The less deformed and tilted Vendian and Lower Paleozoic beds overlie the late Riphean strata on an angular unconformity (Kiselev & Korolev 1972, Becker 1987, 1988).

Predominantly north vergent folds in the middle and late Riphean rocks have consistent orientations; their axes are subhorizontal trending 100–110°. The axial planar cleavage distribution across the Precambrian rock sequences demonstrates distinct zoning (Becker *et al.* 1991). Spaced smooth and rough cleavages in the middle Riphean strata cut all the rock units. The lower part of the late Riphean sequence is characterized by a disjunctive rough cleavage which appears mainly in the clastic rocks. In shales and siltstones of the uppermost Riphean strata the disjunction cleavage is generally anastomosing.

Oriented specimens were taken along a section located in the central part of the Uzunakhmat Sheet (Figs 1c & d). The section crosses the southern flank of a synclinal fold, from the trough and to the steeply inclined limb. The crest of the adjacent anticline is cut by a reverse fault (Fig. 1c). An increase in mesoscopic-scale deformation toward the steep limb of the syncline was observed in the decreasing width of microlithons and increasing flatness of detrital grains along the cleavage plane. The cleavage orientation which remains constant across the section (dip angle 70–75°, towards 195–200° Fig. 1d) forms a significant angle with bedding in the trough segment of the syncline, whereas it is almost parallel to bedding in the southern flank of the syncline.

METHODS

The sandstones of the Uzunakhmat Formation have a pronounced lineation, defined by flattened detrital grains aligned parallel to fold axes (Khudoley 1993), and lying within the cleavage plane. If, as is commonly accepted, cleavage develops parallel to the XY plane of the finite strain ellipsoid (Cloos 1947, Hobbs 1971, Siddans 1972, Wood 1974, Groshong 1975, Murphy 1990), then the orientation of the principal axes of finite strain is as following: X is the extension axis (lineation),

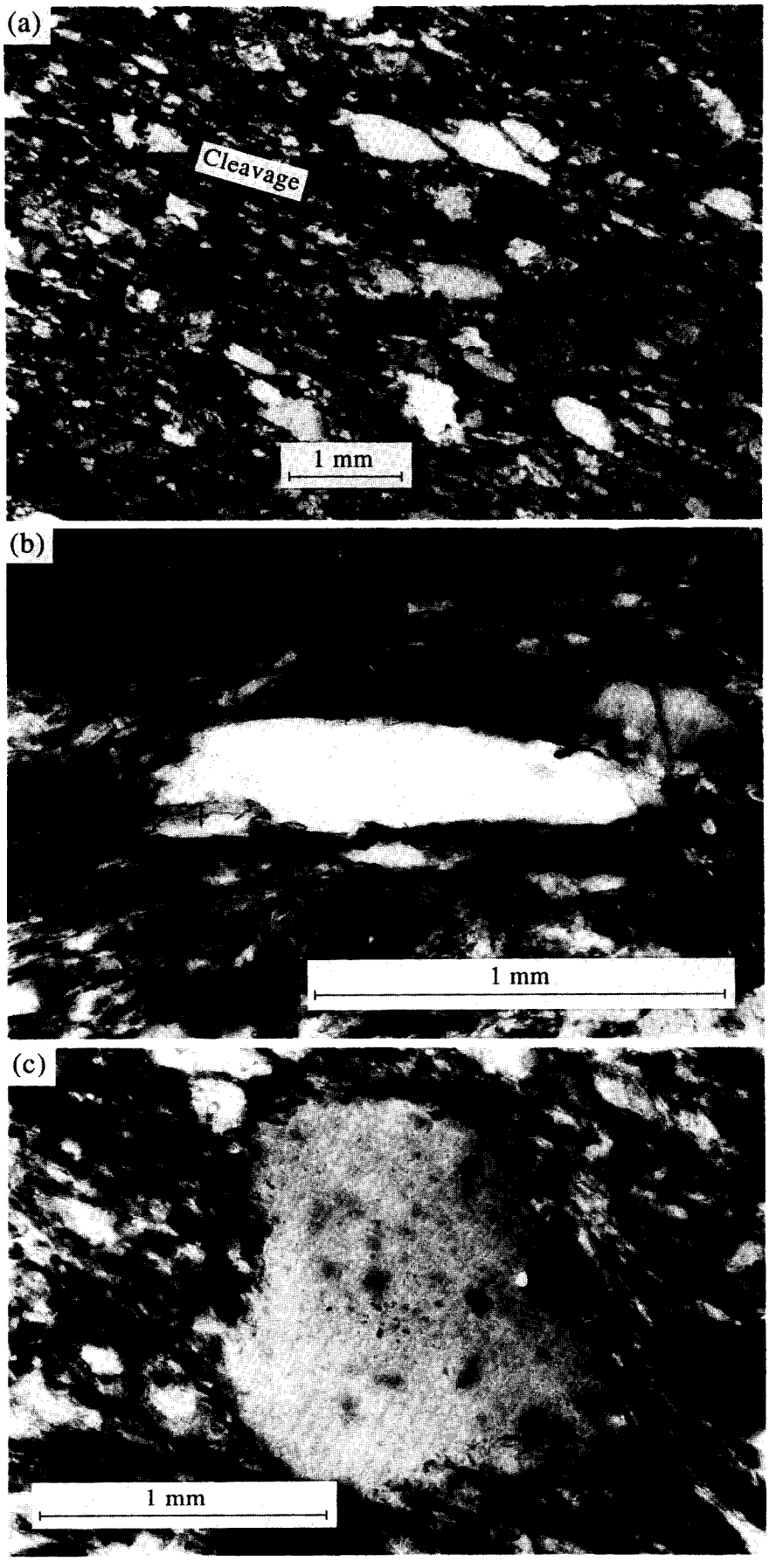

Fig. 2. Photomicrographs of cleaved sandstones. (a) Alignment of fine-grained phyllosilicates (chlorite, muscovite) defining a pervasive schistosity. The majority of detrital grains are flattened and truncated against the cleavage. (b) Very thin, flattened pressolved detrital quartz (X-grains) with smooth sides aligned parallel to the cleavage. (c) Grains showing only slightly modified detrital shapes (Z-grains). Such grains have rounded or irregular boundaries against the cleavage and exhibit long tails of pressure shadows.

Z (the axis of shortening) is perpendicular to the cleavage plane, and Y (the intermediate axis) lies in the cleavage plane normal to the lineation. An orthogonal pair of oriented thin sections was prepared for each specimen, in planes perpendicular to the cleavage, and oriented parallel and perpendicular to the mineral lineation. The sections oriented parallel to the mineral lineation (XZ sections) display a strong elongation of detrital grains parallel to the cleavage, whereas in the sections perpendicular to the mineral lineation the samples either do not show preferred grain orientation, or show a very small elongation in the cleavage plane. The orientation of c-axes and the aspect ratios of the detrital quartz grains were measured in the XZ sections.

Three parameters were measured for each detrital grain of quartz in XZ sections: (1) Lx—the length along a cleavage plane (in most cases coinciding with the grain elongation); (2) Lz—the width of the grain perpendicular to the cleavage; and (3) Cv—orientation of c-axes. Linear measurements were taken along lines across the middle of the grains. Thin-sections were traversed with a grid with the distance between scan-lines 1.0–1.2 mm. All detrital grains with a diameter exceeding 0.2 mm were measured, whereas smaller grains were skipped in order to avoid confusion with recrystallized quartz grains. The aspect ratio (Lx/Lz) and the angle between the c-axis and Z axis of shortening ($Cv \wedge Z$) were calculated for each grain. Orientations of c-axes were measured on a universal stage. These orientations were taking directly c-axes that form an angle of 0–40° with the axis of symmetry of a microscope. In cases in which the c-axes formed a large angle with the axis of symmetry of a microscope (50–90°), the measured element was the circular section perpendicular to c-axis. Both the circular sections and the c-axes were measured several times for grains forming an angle of 40–50° with the axis of symmetry of a microscope, and the mean positions of the c-axis were determined. The last procedure allowed the errors in this interval to decrease.

MICROSTRUCTURES

The rocks examined consist of detrital grains, recrystallized quartz, albite, and phyllosilicates. A pervasive schistosity is defined by the alignment of fine-grained phyllosilicates of chlorite and muscovite (Fig. 2a). Detrital components are quartz (60–70%), feldspars (10–20%), chert, quartzite (10–15%) and felsic volcanics (5–10%). Grain size ranges from 0.1 to 1.2 mm along the maximum dimension. The majority of detrital grains show an abrupt truncation along cleavage planes, whereas many grains exhibit fibrous tails (pressure shadows) extending parallel to the cleavage. The planar grain boundaries which terminate at cleavage planes and the redeposition of removed quartz into pressure shadows indicate that pressure solution was the major mechanism for modifying detrital grain shapes (Groshong 1976, Onasch 1983). Recrystallized quartz in the rock matrix forms thin platelike grains (10–70 μm along the maximum dimension) which are aligned parallel to the cleavage. The amount and size of recrystallized quartz grains increases from specimen K1-87 to specimen K4-87, i.e. in the direction to the steep limb of the syncline (Fig. 1d). The mean aspect ratio of the pressolved quartz increases in the same direction.

The cleavage in specimens K1-87 and K2-87 is rough (classification of Powell 1979) with strong preferred orientation of phyllosilicates and a pronounced shape elongation of detrital grains. The cleavage in specimen K3-87 and K4-87 is transitional from rough to spaced disjunctive with a well developed domainal structure. Cleavage domains consist of oriented fine flakes of chlorite and muscovite, their widths ranging from 0.03 to 0.1 mm in specimen K3-87, and increasing up to 0.5 mm in specimen K4-87.

The orientation of c-axes of detrital quartz is shown in Fig. 3. Quartz grains in weakly-deformed sandstones (specimens K1-87 and K2-87) display a slight preferred orientation of the c-axes. Maxima, situated at 40–50° to the Z axis, are symmetrical with respect to the (XY) cleavage. More deformed sandstones (K3-87 and K4-87) do not exhibit any distinct orientation of c-axes. The absence of any obvious c-axis preferred orientation with increasing strain is particularly noticeable.

The majority of detrital grains are flattened and truncated against the enveloping cleavage. The amount of truncation varies significantly between the grains. Two end-member groups of pressolved grains can be identified in each specimen. The grains of the first group (X-grains) display the highest degree of pressure solution. The grains are very thin, flattened (aspect ratio of 4.0 and more), and have smooth sides aligned parallel to the cleavage (Fig. 2b). Grains of the second group (Z-grains) preserve only slightly modified detrital shapes. They are almost equant and have long tails of pressure shadows (Fig. 2c). The orientation of c-axes of the X- and Z-grains has been measured in thin section K2-87 (Fig. 3b). The X-grains (crosses in Fig. 3b) are preferentially concentrated around the maxima of the detrital quartz c-axes, whereas Z-grains (dots in Fig. 3b) tend to fill spaces beyond the maxima. A histogram showing the relative frequency of X- and Z-grains via the c-axes angle to Z-axis is given in Fig. 4. The amounts of X- and Z-grains, in each interval of $Cv \wedge Z$, were normalized to the total amount of c-axes of detrital quartz measured at this interval. This procedure was used because the numbers of grains in different intervals of $Cv \wedge z$ varied significantly (Fig. 5). If the Cv-axes of quartz are distributed randomly, the number of cases in which the Cv-axis form a small angle with the Z-axis is significantly smaller than the number of cases in which the Cv-axis form a high angle with the Z-axis. This can be demonstrated on a sphere (Fig. 6): the frequencies of randomly oriented axes, measured at different angular intervals relative to an arbitrary line, correlate as squares of surfaces of spherical segments between small circles (parallels), which bound these intervals. In turn, the squares of the spherical segments correlate in the same way as ratio of the projections of the segments on this line. Any signifi-

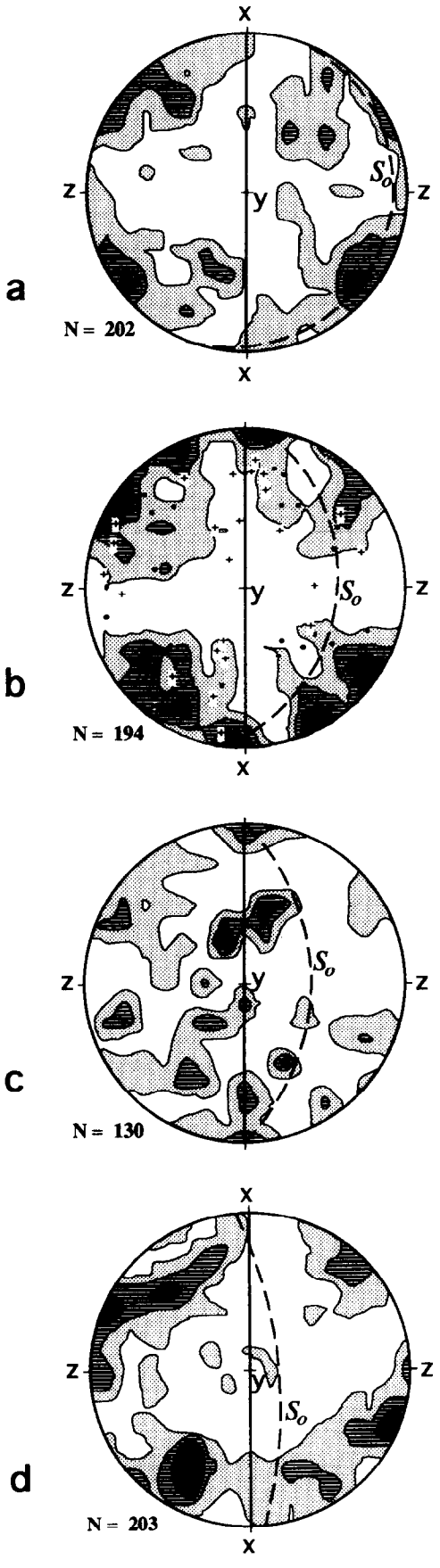

Fig. 3. Fabric diagrams of c-axis of the detrital quartz. Dots are c-axis of X-grains and crosses are c-axis of Z-grains. X is the axis of extension, Z is the axis of shortening, XY (solid line) is the cleavage plane, S_0 (dashed line) is the bedding plane. (a) Specimen K1-87; (b) specimen K2-87; (c) specimen K3-87; (d) specimen K4-87. Equal-angle lower-hemisphere projection; contours 1, 2, 3, 4%.

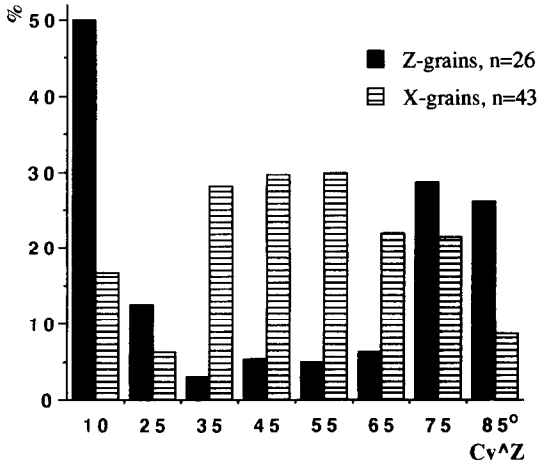

Fig. 4. Histogram showing the relative frequency of X- and Z-grains versus the angle $Cv \wedge Z$ for the specimen K2-87. The relative frequency was calculated as the ratio of the X- and Z-number of grains to the population number of all measured grains within a specified interval.

cant deviation from the theoretical distribution indicates a preferred orientation.

The main distinguishing feature of the frequency distribution (Fig. 4) is that the majority of X-grains have the angles $Cv \wedge Z$ between 30 and 60° with alignments up to 80° also manifested. On the other hand, Z-grains tend to have c-axes either parallel (angles $Cv \wedge Z$ 0–20°) or perpendicular to the Z direction (70–90°). The distribution of these two end-member groups shows the dependence of the amount of pressure solution to the angular relationship between c-axes of the grains and Z-axis of shortening.

RESULTS AND DISCUSSION

A plot of the aspect ratios as a function of $Cv \wedge Z$ for all specimens is given in Fig. 7. The points show a scatter in a wide range of aspect ratios, but smaller aspect ratios are seen for small angles of $Cv \wedge Z$ (0–20°). The means of aspect ratios, calculated for intervals of 10° of $Cv \wedge Z$, are plotted as triangles in the same graphs. Each specimen reflects a similar dependence of the mean aspect ratio on the angle $Cv \wedge Z$. Grains of small $Cv \wedge Z$ angles show the lowest mean aspect ratio, and grains having $Cv \wedge Z$ within 40–50° to Z show the highest mean aspect ratio. A consecutive increase in mean aspect ratios toward the central portion of the graph ($Cv \wedge Z$ = 40–50°) is observed. Wide standard deviations increase the 95% confidence intervals for means, and make the observed trend less obvious.

Two major factors control the standard deviation of the aspect ratios. The first is related to the original elongation of detrital grains. Sandstones of the Uzunakhmat Formation are poorly sorted and laminated, being a part of turbiditic sequence (Korolev & Maksumova 1964, Maksumova 1967). A wide spectrum of shape orientations of the grains that preserved their original shape has been noted in the slightly deformed sandstones of specimens K1-87 and K2-87. Therefore,

the aspect ratio of pressolved grains should reveal a broad range, in response to the original dimension and orientations with respect to the cleavage plane, as shown in Figs. 8(a) & (b). Indeed, the standard deviation of aspect ratios of pressolved grains should remain the same as the standard deviation of aspect ratios of nondeformed grains, measured in the same directions. Thus, if the pressure solution is equal at different angles of $Cv \wedge Z$, the graph of the aspect ratios versus $Cv \wedge Z$ would represent a wide band parallel to the $Cv \wedge Z$ axis, and shifted up along the Lx/Lz axis (Fig. 8c). If the amount of pressure solution differs at different angles of $Cv \wedge Z$, this band should be curved, whereas the deviations from means of Lx/Lz should remain the same with changing angle of $Cv \wedge Z$ (Fig. 8d). The difference in aspect ratios between two intervals of $Cv \wedge Z$, may be significant within a selected level of significance, but only if the difference in pressure solution exceeds the sizes of the confidence intervals for means, which in turn depend upon the standard deviation of the aspect ratios of the original grains. A slight preferred grain elongation within the bedding plane (if such existed) may have played a minor role in the observed distribution, inasmuch as the cleavage forms significant angles with the bedding plane. This angle varies from sample K1-87 to sample K4-87, whereas the relationship between $Cv \wedge Z$ and aspect ratios remains the same throughout the sample sequence.

The second factor which may increase the standard deviation of the aspect ratios is the error of measurements. Strong mineral lineation in the plane of cleavage, parallel to subhorizontal fold axes makes the measurements of aspect ratios in the section XZ appropriate. Nevertheless, a slight obliquity of a grain to a thin-section plane introduces measurement errors of long and short axes: grain elongation may vary significantly in the thin section. Such measurement errors lead to a wider scatter of the aspect ratios, but this scatter should be the same at different angles of $Cv \wedge Z$, and therefore the difference in mean aspect ratios depends upon other factors.

The graphs of mean aspect ratios (Fig. 7) approximate lines convex upward and having a single peak at the interval of $Cv \wedge Z$ of 40–50°. To test whether parabolic approximations are significant to this distribution, a quadratic regression was applied to the data. Two statistical hypotheses were tested by the quadratic regression: (1) is the regression significant? (or in other words, is the variance constant about the regression line?) and (2) is the quadratic term making a significant contribution to the regression? (or in other words, is the observed maximum at the central portion of the axis $Cv \wedge Z$ statistically significant?) (Zar 1984, Davis 1986).

The quadratic regression (Fig. 9, Table 1) shows that it is an appropriate model for all four samples ($F = 5.33$–11.09, $p = 0.0055$–0.0001), and that the quadratic regression is a highly significant improvement over the linear regression (partial F of the quadratic term ranges from 10.6 to 21.9, t-value ranges from 3.26 to 4.67, $p = 0.0013$–0.0001). Plots of residuals (Fig. 9b) show that they form a uniform band around the regression line, exhibiting homoscedasticity. The Durbin–Watson stat-

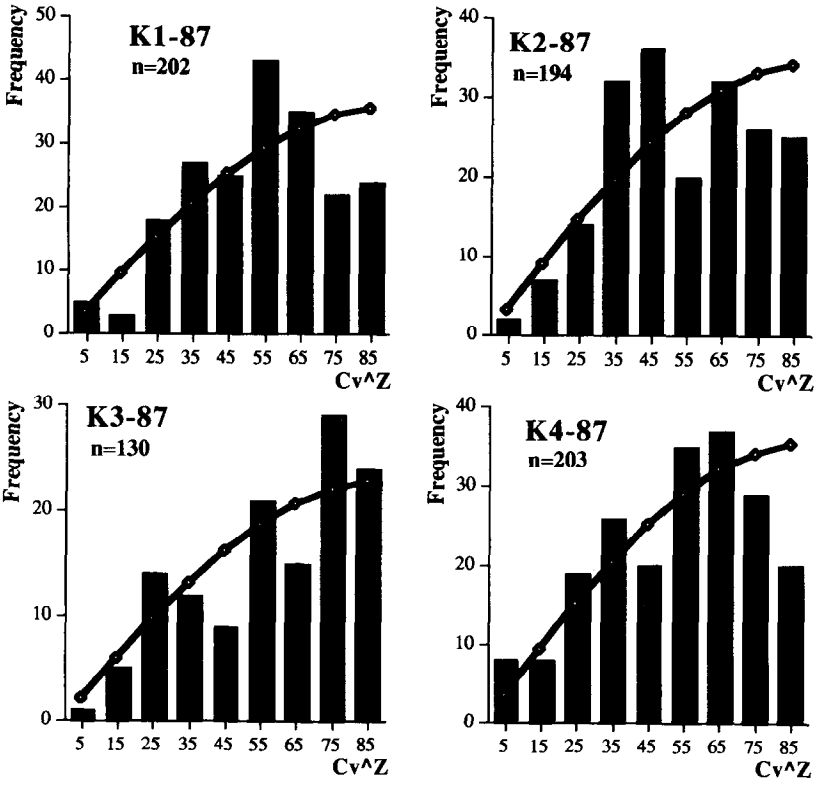

Fig. 5. Histograms showing the relative frequency of c-axes at 10° angular intervals of $Cv \wedge Z$ for specimens K1-86 and K4-87. Solid line shows the expected theoretical distribution for random c-axes orientation. Samples K3-87 and K4-87 show distributions that are closer to the theoretical one.

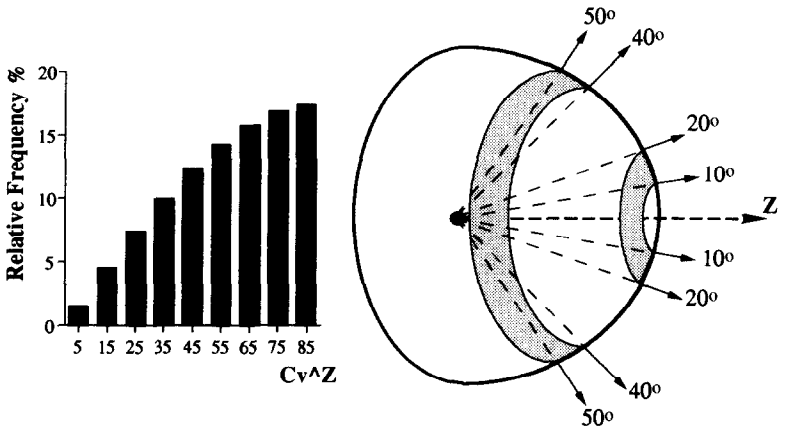

Fig. 6. A scheme (right) demonstrating the difference in frequency of randomly oriented linear elements, measured at different angles to the arbitrary line (Z). The frequency histogram (left) shows theoretically expected distribution for randomly oriented c-axes measured through intervals of 10° of $Cv \wedge Z$.

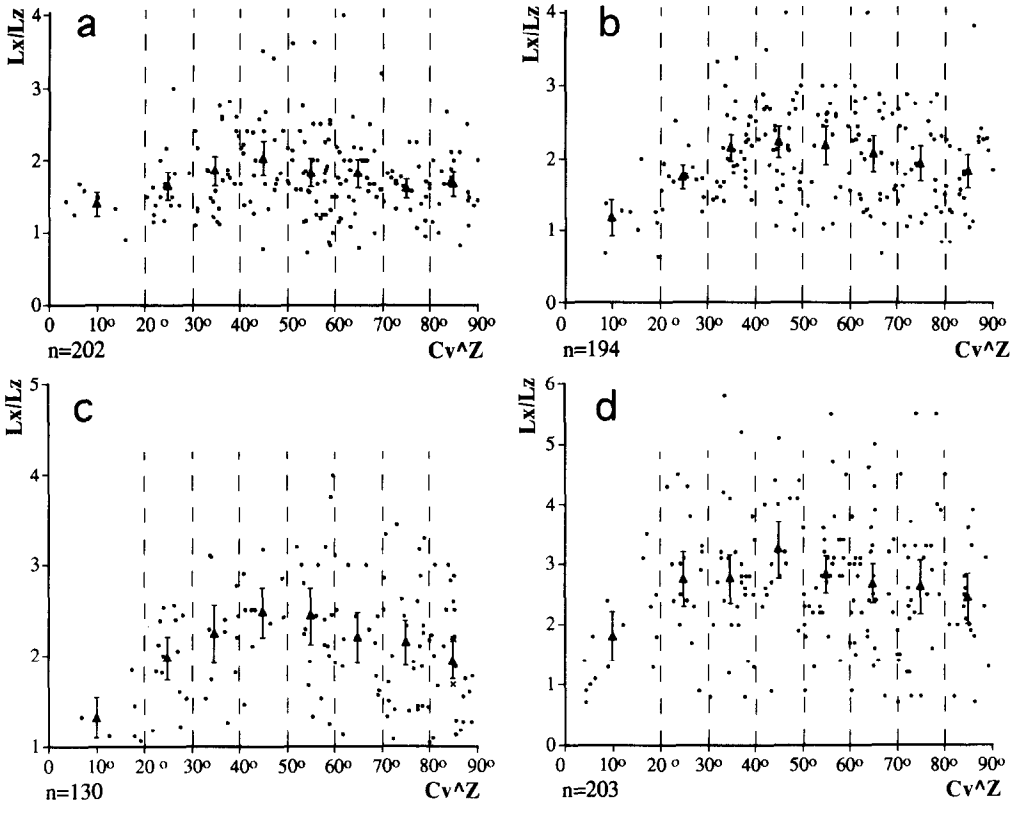

Fig. 7. Plot of aspect ratios (Lx/Lz) of detrital quartz grains versus the $Cv \wedge Z$ angle. The mean aspect ratios through intervals of 10° of $Cv \wedge Z$ (dashed vertical bars) are shown as triangles (the first interval unites data of 0–20° of $Cv \wedge Z$, as the amount of grains having small $Cv \wedge Z$ angles was too small). Vertical bars show 95% confidence intervals for calculated means.

istics are close to 2 (Table 1), demonstrating that the residuals are not autocorrelated. Normal probability plots (Fig. 9c) indicate that the residuals are normally distributed.

The quadratic regression (Fig. 9, Table 1) demonstrates that quartz grains, oriented at small angles between c-axis and the Z-axis of shortening, are most resistant to pressure solution. Grains aligned at 45–55° to Z show the highest amounts of pressure solution. A maximum value of the aspect ratio, based on the coefficients of fitted quadratic equations, ranges from 50.9 to 54.5° (Table 1). This conclusion is supported by the difference of distribution of Z- and X-grains which represent the lowest and highest members of the pressure solution series (Fig. 4).

The typical crystal shape of α-quartz and the angular relationships of the mean faces to the c-axis are shown in Fig. 10. By comparing the crystallography of quartz with the patterns in analyzed graphs we observe that the c-axis (0001) direction is the one most stable to pressure solution in quartz crystal, whereas rhombohedrons $r(10\bar{1}1)$, $z(01\bar{1}1)$ and trigonal dipyramids $\varepsilon(2\bar{1}\bar{1}2)$ are the most unstable, comprising the faces most easily soluble during deformation.

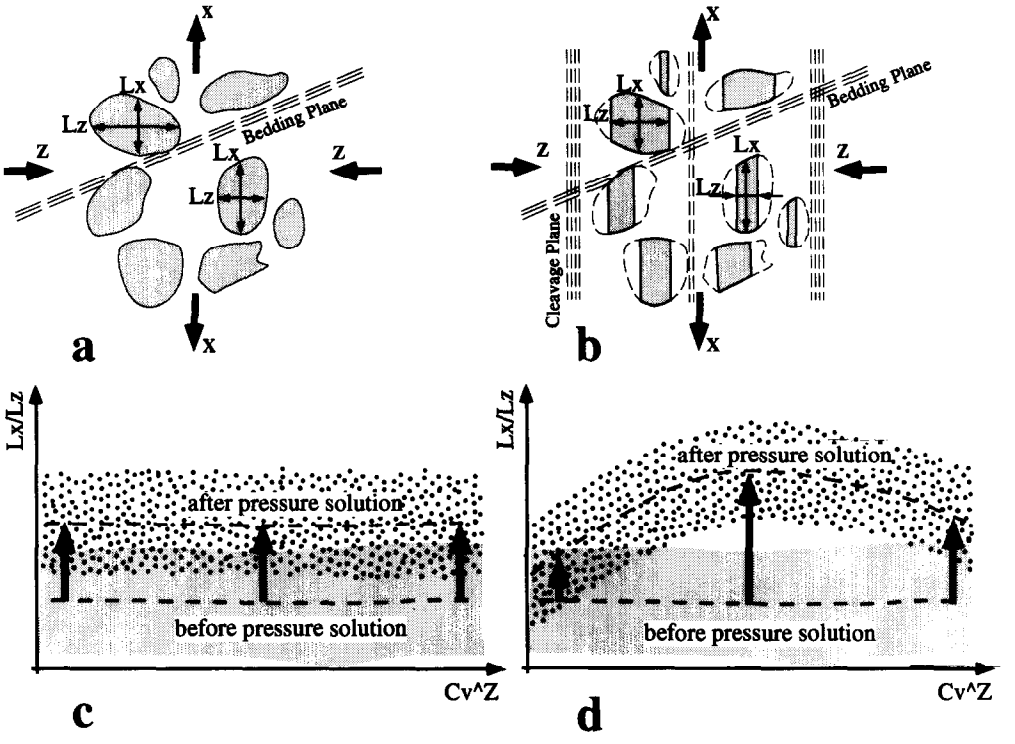

Fig. 8. Scheme showing pressure solution of detrital grains that originally had various shapes and were arranged at random directions. (a) Sand grains before pressure solution; (b) the same grains after pressure solution. (c) Schematic graph of *Lx/Lz* versus *Cv* ^ *Z*, showing the case when the pressure solution is equal at different angles of *Cv* ^ *Z*. The graph represents a wide band parallel to the *Cv* ^ *Z* axis and is shifted up along the *Lx/Lz* axis. (d) Schematic graph showing a case in which the amount of pressure solution differs at different angles of *Cv* ^ *Z*. The band of points is curved, whereas the deviations from means of *Lx/Lz* remain the same with changing angle of *Cv* ^ *Z*.

CONCLUSIONS

This study of the relationship between crystallographic orientation and pressure solution in quartz shows the following:

(1) Quartz offers variable resistance to pressure solution along different crystallographic directions.

(2) Quartz grains with a small angle between *c*-axis and the *Z*-axis of shortening exhibit the least amount of pressure solution, whereas grains with *c*-axis aligned about 50° to *Z* manifest the highest degree of pressure solution.

(3) The *c*-axis (0001) direction is the one most resistant to pressure solution in a quartz crystal, whereas rhombohedrons and trigonal dipyramids are the most easily soluble faces during deformation.

Table 1. Completed ANOVA for significance of the quadratic regression of aspect ratios on the *Cv* ^ *Z* angle for samples K1-87–K4-87

	Analysis of variance								
	Regression			Residual					
Specimen	Degrees of freedom	Sum of squares	Mean square	Degrees of freedom	Sum of squares	Mean square	Durbin–Watson statistic	*F*-test	Probability
K1-87	2	3.146	1.573	199	58.823	0.296	2.098	5.332	0.0055
K2-87	2	8.338	4.169	191	71.81	0.376	1.971	11.088	0.0001
K3-87	2	7.759	3.88	127	47.934	0.377	1.735	10.279	0.0001
K4-87	2	14.469	7.234	200	222.327	1.112	1.678	6.508	0.0018

	Beta Coefficients											
		β_1					β_2					
Specimen	Intercept (α)	Value	Standard error	*t*-Value	Partial *F*	Probability	Value	Standard error	*t*-Value	Partial *F*	Probability	Maximum
K1-87	1.211	0.0267	0.00847	3.151	9.914	0.0019	−2.615E-4	8.022E-5	3.26	10.626	0.0013	50.94
K2-87	0.76	0.053	0.011	4.692	22.011	0.0001	−4.889E-4	1.044E-4	4.681	21.916	0.0001	54.30
K3-87	0.71	0.0623	0.014	4.517	20.436	0.0001	−5.714E-4	1.266E-4	4.509	20.335	0.0001	54.56
K4-87	1.452	0.0552	0.01532	3.601	12.966	0.0004	−5.24E-4	1.517E-4	3.453	11.921	0.0007	52.63

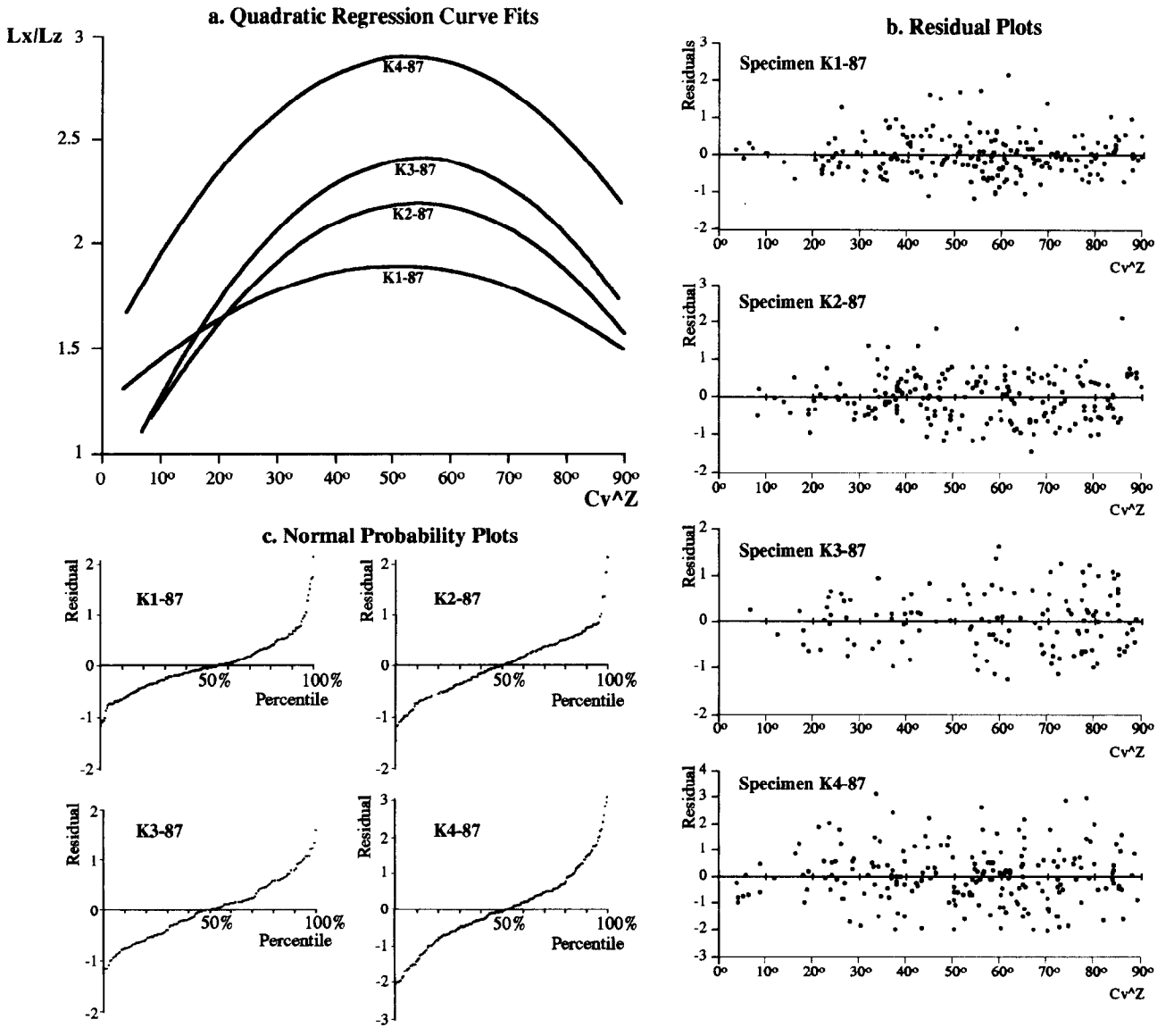

Fig. 9. Quadratic regression analysis of aspect ratios on the $Cv \wedge Z$ angle for samples K1-87–K4-87.

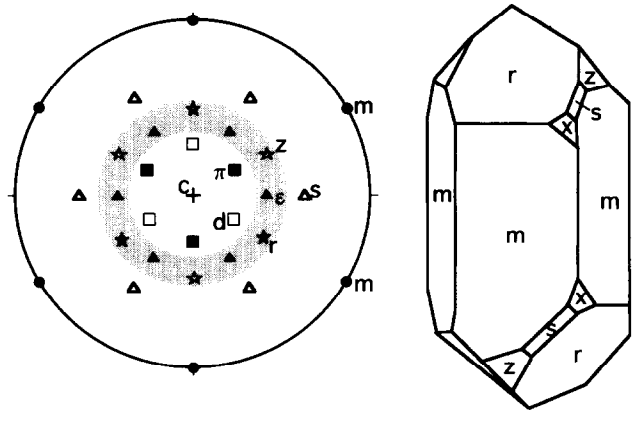

Fig. 10. A typical crystal of α-quartz (right) and the angular relationship of main faces with the *c*-axis (left). The area between 45 and 55° to the *c*-axis is shaded. Faces: $r(10\bar{1}1)$, $z(01\bar{1}1)$, $d(10\bar{1}2)$ and $\pi(01\bar{1}2)$—rhombohedrons; $m(10\bar{1}0)$—prisms; $s(1121)$ and $\varepsilon(2\bar{1}\bar{1}2)$—trigonal dipyramids; $x(51\bar{6}1)$—trigonal trapezohedron.

Acknowledgements—Field studies were carried out during geological mapping under financial and technical support by Northern Kyrgyzian Geological Expedition. The use of facilities at Ramon Science Center and Geological Department of Ben-Gurion University in the Negev is gratefully acknowledged. I would like to thank Arie Shimron and Emanuel Mazor for their constructive suggestions and for improving the English. This paper was improved by comments and suggestions of C. M. Onasch and J. P. Evans.

REFERENCES

Bakirov, A. & Dobrezov, N. L. 1972. *Metamorphic Complexes of the Eastern Part of Central Asia.* Ilim, Frunze (in Russian).

Becker, A. 1987. On the relationships between tectonic structures of the Uzunakhmat and the Karagoin blocks of the Talas-Karatau zone (Northern Tien Shan). In: *Caledonides of Tien Shan* (edited by Korolev V. G.). Ilim, Frunze, pp. 21–36 (in Russian).

Becker, A. 1988. Evolution of the deformation processes in the central part of the Talas–Karatau structural-formation zone (Northern Tien Shan) during the Precambriam and the Early Paleozoic. *Izvestia Acad. Nauk Kazakhskoi S.S.R.* **2**, 44–53 (In Russian).

Becker, A., Konuhov, A. A. & Slotuk, B. M. 1991. Folding in Talas ridge, its zoning and stages of evolution. In: *Tectonofacial Analysis and Its Role in Geology, Geophysics and Metalogeny* (edited by Patalakha E. I.). Gylym, Alma-Ata, 107–112 (in Russian).

Bouchez, J. L. 1978. Preferred orientation of <*a*> axes in some tectonites: kinematics inferences. *Tectonophysics* **49**, 725–750.

Brace W. F. 1960. Orientation of anisotropic minerals in a stress: discussion. *Mem. geol. Soc. Am.* **79**, 9–20.

Cloos, E. 1947. Oolite deformation in the South Mountain folds, Maryland. *Bull. geol. Soc. Am.* **89**, 481–493.

Davis, J. C. 1986. *Statistics and Data Analysis in Geology*. John Wiley & Sons, NY.

Delizin, I. S. 1976. About real and simulated stable thermodynamic orientation of quartz in a quartzite. *Izvestia Academii Nauk SSSR, Seria Geologicheskaia* **1**, 109–124 (in Russian).

DeBoer, R. B. 1977. Pressure solution: theory and experiments. *Tectonophysics* **39**, 287–301.

Dewers, T. & Ortoleva, P. 1991. Influences of clay minerals on sandstone cementation and pressure solution. *Geology* **19**, 1045–1048.

Durney D. W. 1972. Solution-transfer, an important geological deformation mechanism. *Nature* **235**, 315–317.

Frolova, N. S. 1982. Influence of metamorphism on deformational properties of rocks (an example from Talas Alatau). *Geotectonika* **4**, 18–24 (in Russian).

Gray, D. R. 1982. Cleavage in psammatic rocks. In: *Atlas of Deformational and Metamorphic Rock Fabrics* (edited by Borradaile, G. J., Bayly, M. B. & Powell, C. McA.). Springer-Verlag, Berlin, 112–113.

Groshong, R. H. 1975. 'Slip' cleavage caused by pressure solution in a buckle fold. *Geology*, **3**, 411–413.

Groshong, R. H. 1976. Strain and pressure solution in the Martinsburg Slate, Delaware Water Gap, New Jersey. *Am. J. Sci.* **276**, 1131–1146.

Hicks, B. D., Applin, K. R., Houseknecht, D. W. 1986. Crystallographic influences on intergranular pressure solution in a quartzose sandstone. *J. sedim. Petrol.* **56**, 784–787.

Hobbs, B. E. 1968. Recrystallization of single crystal of quartz. *Tectonophysics* **6**, 353–401.

Hobbs, B. E. 1971. The analysis of strain in folded layers. *Tectonophysics* **11**, 329–375.

Hobbs, B. E. 1985. The geological significance of microfabric analysis. In: *Preferred Orientations in Metals and Rocks: An Introduction to Modern Texture Analysis* (edited by Wenk, H.-R.). Academic Press, NY, 463–484.

Houseknecht, D. W. 1984. Influence of grain size and temperature on intergranular pressure solution, quartz cementation, and porosity in a quartzose sandstone. *J. sedim. Petrol.* **54**, 348–361.

Houseknecht, D. W. 1988. Intergranular pressure solution in four quartzose sandstones. *J. sedim. Petrol.* **58**, 228–246.

Kamb, W. B. 1959. Theory of preferred crystal orientation developed by crystallization under stress. *J. Geol.* **67**, 153–170.

Kazakov, A. N. 1987. *Dynamic Analysis of Microstructural Orientations of Minerals*. Nauka, Leningrad (in Russian).

Kennedey, G. C. 1950. A portion of the system silica–water. *Econ. Geol.* **45**, 629–653.

Khudoley, A. K. 1993. Structural and strain analysis of the middle part of the Talassian Alatau ridge (Middle Asia, Kirgizstan). *J. Struct. Geol.* **12**, 693–706.

Kiselev, V. V. & Korolev, V. G. 1972. *Precambrian Tectonics of the Central Asia and Central Kazakhstan*. Ilim, Frunze (in Russian).

Kiselev, V. V. & Korolev, V. G. 1981. *Paleotectonics of the Tien Shan Precambrian and Lower Paleozoic*. Ilim, Frunze (in Russian).

Kiselev, V. V., Apayarov, F. H. & Becker, A. 1988. The Epibaicalic Precambrian of Tien Shan. In: *The Precambrian and the Lower Paleozoic of Tien Shan* (edited by Kiselev, V. V.). Ilim, Frunze, 127–143 (in Russian).

Korolev, V. G. & Maksumova, R. M. 1964. The Late Precambrian of Talas Alatau. *Proc. Frunze Politechnical Institute*, **24** (in Russian).

Maksumova, R. A. 1967. The Late Riphean formations of Talas ridge. In: *Formations of the Late Precambrian and the Early Paleozoic of Northern Kyrgyzstan*. Ilim, Frunze, 23–35 (in Russian).

Maksumova, R. A. 1980. *Baikalian Orogenic Complex of the Northern Tien Shan and Southern Kazakhstan*. Ilim, Frunze (in Russian).

Murphy, F. X. 1990. The role of pressure solution and intermicrolithon-slip in the development of disjunctive cleavage domains: a study from Helvick Head in the Irish Variscides. *J. Struct. Geol.* **12**, 69–81.

Onasch, C. M. 1983. Origin and significance of microstructures in sandstones of the Martinsburg Formation, Maryland. *Am. J. Sci.* **283**, 936–966.

Powell, C. McA. 1979. A morphological classification of rock cleavage. *Tectonophysics* **58**, 21–34.

Price, J. P. 1985. Preferred orientations in quartzites. In: *Preferred Orientations in Metals and Rocks: An Introduction to Modern Texture Analysis* (edited by Wenk, H.-R.). Academic Press, NY, 385–406.

Price, N. J. & Cosgrove, J. W. 1990. *Analysis of Geological Structures*. Cambridge University Press.

Renton, J. J., Heald, M. T. & Cecil, C. B. 1969. Experimental investigation of pressure solution of quartz. *J. sedim. Petrol.* **39**, 1107–1117.

Siddans, A. W. 1972. Slaty cleavage—a review of research since 1815. *Earth Sci. Rev.* **8**, 205–232.

Sobolev, S. V. 1957. On the pecularities of mineral crystallization under stress. *Mineralogical Bulletin of Lvov Geological Society*, **11**, 45–51 (in Russian).

Soper, N. J. 1986. Geometry of transecting, anastomosing cleavage in transpression zones. *J. Struct. Geol.* **8**, 937–940.

Taylor, J. M. 1950. Pore-space reduction in sandstones. *Bull. Am. Assoc. Petrol. Geol.* **57**, 547–564.

Twiss, R. J. & Moores, E. M. 1992. *Structural Geology*. Freeman, NY.

Waldron, H. M. & Sandiford, M. 1988. Deformation volume and cleavage development in metasedimentary rocks from the Ballarat slate belt. *J. Struct. Geol.* **10**, 53–62.

Wood, D. S. 1974. Current views on the development of slaty cleavage. *Earth Sci. Rev.* **2**, 1–37.

Zar, J. H. 1984. *Biostatistical Analysis*. Prentice-Hall International, Englewood Cliffs.